Micro-Structural Characterization of Cast Mg-TiC MMC's

A. Munitz[#1], I. Jo[*2], J. Nuechterlein[*2], W. Garrett[*2], J.J. Moore[*2], M.J. Kaufman[*2]

#1Nuclear Research Center-Negev,P.O.Box 9001, Beer-Sheva, 841900, ISRAEL

[2*] Department of Metallurgical and Materials Engineering,Colorado School of Mines, Golden, Colorado, USA

Abraham Munitz <unitza@yahoo.com>,Ilguk Jo <ijo@mymail.mines.edu>

Jacob Nuechterlein jnuechte@mines.edu,William Garrett wgarrett@mines.edu

John J Moore jjmoore@mines.edu,Michael J Kaufman <mkaufman@mines.edu>

***Abstract*-Mg-based MMCs containing 10, 20 and 30 vol. % TiC were produced by stirring cold pressed pellets containing micron-size TiC (80 vol. %) and Mg (20 vol. %) powders into molten Mg-9 wt.% Al and casting to produce small billets. These composites were characterized in the as-cast condition and after solution treating and aging using SEM/EDS. Micro-hardness measurements were used to correlate with the microstructures. The as-cast composites consist of Mg-Al dendrites and interdendritic regions are comprised of TiC particles as well as $Mg_{17}Al_{12}$, Mg and Al oxides, and porosity. Isolated TiC agglomerates resulting from incomplete "disintegration" of the TiC pellets were also observed. The oxides and porosity were best near the top of the billets. A solution heat treatment was used to homogenize the matrix and decrease the $Mg_{17}Al_{12}$ and oxides without noticeably affecting the TiC. Aging at 210°C caused micro-structural and hardness changes similar to those for AZ-91 alloys.**

Keywords-Metal Matrix Composites (MMCs); Mg-Al Alloys; TiC; Mechanical Properties; Microstructure

I. INTRODUCTION

There is a growing demand in the automotive industry for reducing vehicle weight to increase efficiency and reduce fuel consumption for lower emission levels. This goal can be achieved by replacing various automotive components (e.g., hoods, doors and bodies) with components made from lightweight metals, like Mg or Al alloys, or using higher strength alloys in thinner cross sections. For the former, the most applicable alloys are those based on Mg-Al, such as AZ91, because of their excellent castability, corrosion resistance, and strength at room temperature [1]-[3]. It is well-known that the strength of the Mg-Al alloys is improved as the Al content increases [4]. Nevertheless, the ductility decreases significantly with increased Al content, which limits the applications of these alloys to less than 9 wt% Al. However, compared to other structural metals, magnesium alloys have a relatively low absolute strength, especially at elevated temperatures, as their applications are usually limited to temperatures of up to 120°C. Further improvements in their high-temperature properties should greatly expand their industrial application [5]. These demands have led to extensive R&D efforts to develop magnesium matrix composites and cost-effective fabrication technologies. For instance, the magnesium matrix composite unidirectionally reinforced by continuous carbon fibbers can readily show a bending strength of 1000 MPa with a density as low as 1.8 g/cm^3 [6]-[7]. The superior mechanical properties can be retained at elevated temperatures of up to 350–400°C [8]-[9]. Another advantage for adding ceramic particles into the Mg alloys is the grain refinement where the particle size affects the matrix grain size and the mechanical properties. For example, Lu et al. [10] showed that a reduction in the SiC size from 50 μm to 10 μm resulted in a grain size change from 43 μm to 23 μm. In general, the use of thermally stable ceramic reinforcements to create Mg based metal matrix composites (MMC) facilitates the retention of enhanced mechanical properties at elevated temperatures [11]. The desirable characteristics of MMCs include enhancements in stiffness, strength, creep resistance, and wear resistance [5]; however, MMCs normally exhibit lower ductility and toughness than the unreinforced matrix [11]. Cao et al. [12], [13] has reported that nanocompositing can actually lead to an increase in the ductility of as-cast magnesium-based metal matrix nanocomposites (MMNCs).

In addition, some Mg alloys such as WE43 are being considered as attractive lightweight materials to manufacture ultra lightweight armoured ground vehicles [14]. The addition of ceramic particles might improve the capability of WE43 for armour applications.

The purpose of this study was to investigate TiC-reinforced Mg alloys using simple casting approaches (e.g. low pressure die casting). The volume fraction and size of the TiC were varied in an effort to characterize its effects on both microstructure and properties

II. EXPERIMENTAL

Pure Mg (99.9%), commercial TiC powder (99.7% purity with grain size of 1~5 μm) and commercial Al powder (99.5 % with average grain size of ~44μm) were used to prepare the Mg-9 wt% Al with 10 to 30 vol.% TiC. The billet dimensions were either 45 or 60 mm diameter and 90 mm height. The amounts of Mg, TiC and the Al were calculated to produce TiC from 10 to 30 vol.%. The TiC and Al powders were weighed according to the desired composition and were mixed using an acoustic vibratory mixer and then they were uniaxially pressed into 12.5 mm diameter cylindrical pellets. The average green density of the pellets was approximately 60% of the theoretical density. The Mg was inserted into boron nitride coated graphite crucible, which was inserted into an iron crucible, which, in turn, was placed in the middle of a 140 kg induction furnace containing an alumina crucible. A protective argon "blanket" was used to cover the melt throughout the entire process to minimize oxidation and the alloy was heated to ~750°C. The molten magnesium was held at 750°C and the desired volume percent of the reinforcement was introduced by submerging the cold pressed pellets into the melt. After their insertion, the "melt" was mechanically stirred for ~5 min using a steel rod to facilitate the

incorporation and uniform distribution of the TiC reinforcement into the melt. During stirring, the temperature was maintained between 750 and 800°C. After stirring, the stirrer was removed and the graphite crucible was extracted and then quenched into water.

The billets containing 10, 20, and 30 vol. % TiC were machined to the desired dimensions and then coated with a commercial 2-part (epoxy / TiB_2 powder) to produce protective coating during the reheating of the billets to above the liquid's temperature of the Mg matrix before placing them into the shot sleeve of an HPDC machine at V-forge die-casting company where they were die cast into either wedge samples or automotive belt tensioning brackets. After casting, the composite materials were heat treated using Mg-AZ91 specifications, i.e. solution heat treated at 413±6°C for 16-24 h, water quenched and then aged at 215±5°C for 5-6 h.

After solidification, the samples were cross-sectioned and prepared using standard metallographic procedures. First, the specimens were abraded on SiC paper to 600 grits and then polished to 1 μm using a diamond paste. After mechanical polishing, the specimens were submerged in a chemical polishing solution and comprised of 100 cc ethanol, 4 cc HNO_3, and 6 cc HCl at room temperature for 5 to 10 sec. Micro-structural examination was performed with scanning electron microscopes (SEM) equipped with energy dispersive spectroscopy (EDS) capabilities. The raw intensity data were corrected with a ZAF computer program [15]. The specimens used for micro-structural examination were also used for Vickers microhardness tests with 1 kg load for 10 s.

For the compression tests, samples with rectangular cross sections were cut with dimensions of 4x4x7 mm. The samples were then compression tested using a crosshead velocity of 1 mm/min.

III. RESULTS AND DISCUSSION

A. Microstructure Examination

A series of backscattered electron images (BEI) illustrating the characteristic microstructure of Mg-9wt.% Al. 10 vol.% TiC are shown in Fig. 1. The microstructure consisted of dark Mg-Al cells matrix (point 4 in Fig. 1b) surrounded by a brighter, higher Z phase (Fig. 1a). First those who need to be solidified are the Mg dendrites which contained up to 9 wt.% Al. The centre of the dendrites is lower in Al and the Al concentration increases towards the interdenritic regions. As solidification proceeds, the TiC particles as well as Al and oxygen are rejected into the interdendritic regions, which solidify last. At higher magnifications, these cells reveal two types of interdendritic microstructures, namely, interdentritic regions which contain a large portion of TiC (Fig. 1a) and those that contain a large portion of $Mg_{17}Al_{12}$ and small amount of TiC (Figs. 1b and 1d). As can be seen in Fig. 1d, the TiC is sometimes embedded in an $Mg_{17}Al_{12}$ phase which is surrounded by an Al- rich layer (about 2 to 3 wt % Al higher than the matrix). EDS analysis indicated the presence of large quantities of oxygen in these regions.

In addition, large areas like point 1 in Fig. 1 can also be seen. At higher magnification (Fig. 1e), this area is observed to consist solely of TiC particles embedded in the Mg matrix with almost no oxides. This is attributed to unintegrated pieces of the TiC pellets which, in spite of the vigorous stirring, did not disperse into the matrix. In contrast, the interdendritic region in Fig. 1f contains a lower density of TiC particles intermixed with $Mg_{17}Al_{12}$ and oxides (Fig. 1f) as well as Mg containing 2 to 3% higher Al than the surrounding matrix (Fig. 1d). Higher magnification of the TiC did not reveal an interaction layer between the TiC and the Mg interface. On the other hand, there were large areas containing interdendritic regions that were composed solely of $Mg_{17}Al_{12}$ as seen in Fig. 1b.

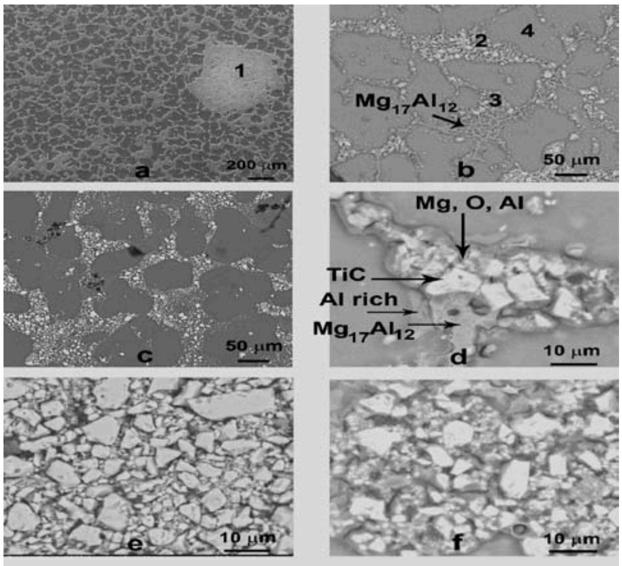

Fig. 1 BEIs illustrating the microstructure of Mg-9wt.%Al + 10 vol.% TiC. (a) overall view; higher magnification of interdendritic regions rich in oxides (b) and TiC (c); (d) higher magnification of the region marked 3 in (b); (e) higher magnification of the region marked 1 in (a); (f) higher magnification of the region marked 2 in (b)

Increasing the TiC in the melt from 10 to 20 vol.% resulted in larger cross-sections of the interdendritic regions and less well developed Mg dendrites (Fig. 2a-b). At 30 vol.% TiC, essentially no dendrite cores were observed (Fig. 2c) although the structure appeared to contain significantly more than 30 vol.% TiC. This has been shown to be an artefact of mechanical polishing [16]. Again, large unintegrated pieces of TiC were also observed in the 30 vol.% TiC material (Fig. 2c).

The effect of solution treatment and aging on the microstructure of the 10 vol.% TiC composite are shown in Fig. 3. Macroscopically, the structure of the Mg dendrites and interdendritic regions could be seen after solution heat treatment. However, microscopic changes associated with aging were too fine to be observed in the SEM images. As expected, the amount of the $Mg_{17}Al_{12}$ phase was reduced although some still existed after the heat treatment. In addition, it appeared that the amount of oxides in the interdendritic regions was reduced by the heat treatment although no attempt was made to quantify this effect. It should be mentioned that, while the majority of the microstructure of the cast billets is similar to that in Figures 1 and 2, there are regions, especially in the upper part of the cast billet near the outer surface, that contain large oxides (the dark phases in Fig. 4). EDS analysis indicated that these oxides contain large O contents as well as a significant amount of sulphur that apparently originated from the TiC powders. The density of the dark particles increased towards the top outer surface. Another type of oxide was found in the interdendritic regions (Figures 1d and 3a-3b). As will be shown below, the oxides reduce the mechanical properties and the workability of the material.

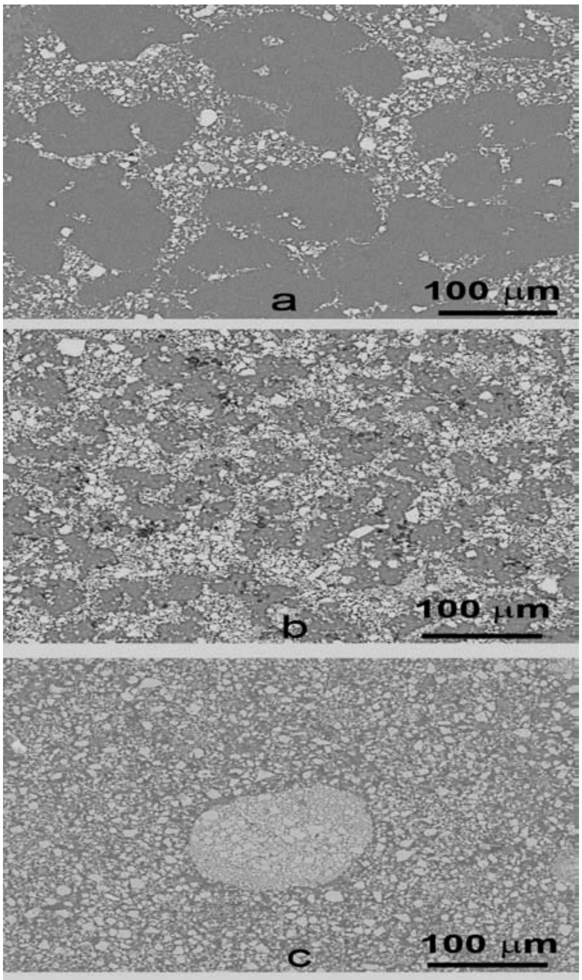

Fig. 2 BEIs illustrating the microstructure of Al-9 wt.% Al as a function of vol.% TiC in the alloy. (a) 10 vol.% (b) 20 vol.% (c) 30 vol.%.

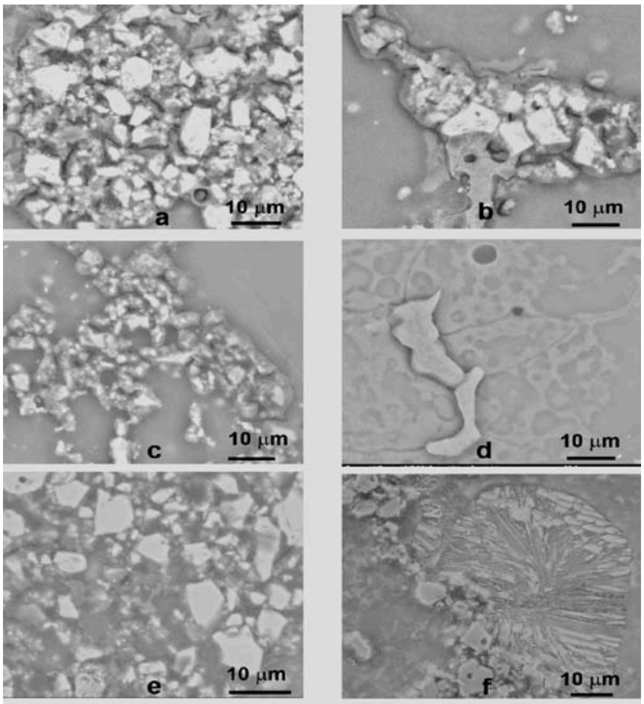

Fig. 3 Backscattered Electron Images (BSE) illustrating the impact of solution treatment and aging on the microstructure of Al-9 wt.% Al-10 Vol.% TiC. **a-b**) As cast, **c-d**) solution heat treated, and **e-f**) aged. (the corrections are bolded).

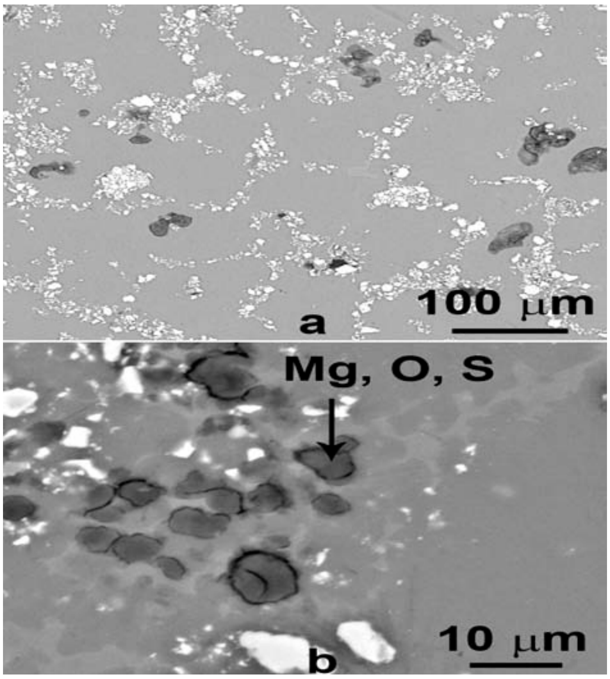

Fig. 4 BEI's of an upper region of the 10 vol. % TiC composite ingot showing the higher density of oxides.

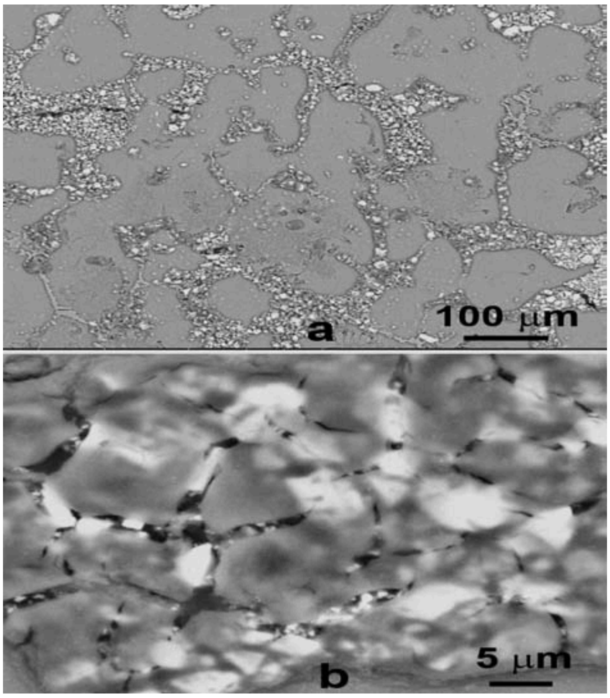

Fig. 5 BEIs of the 10 vol.% TiC composite rolled to 30% thickness reduction at 350oC. a) Low magnification view. b) Higher magnification of interdendritic regions showing microcracks.

Another issue is the uneven distribution of the TiC. While the majority of the billet microstructure is similar to that in Fig. 1c with a relatively even distribution of TiC particles in the interdendritic regions, there are regions in which the interdendritic regions contain continuous $Mg_{17}Al_{12}$ similar to that in Fig. 1b. Also, the regions of un-integrated TiC pellets such as that in Fig. 1a are, in some cases, quite large.

The oxygen in the interdendritic regions plays a central role in the ability of the Mg MMC's to undergo large thickness reduction during hot rolling. For example, a large number of microcracks can be seen in the interdendritic

regions (Fig. 5b) of the 10 vol.% TiC after rolling to 30% thickness reduction at 350°C. These micro-cracks can develop into a fracture as can be seen in Fig. 5a.

B. Mechanical Properties

Compression stress/strain curves illustrating the impact of the TiC reinforcements on an Mg-9 wt % Al matrix are shown in Fig. 6 and a summary of the compression results in Table 1. As can be seen from Fig. 6 and Table 1, the compressive yield strength increased from 110 MPa to 150, 310 and 380 MPa for 10, 20 and 30 vol.% TiC samples, respectively, while the compressive deformation to fracture decreased from 13% to about 2.5% for the 30 vol.% TiC sample. It is also apparent that increasing the volume fraction of the TiC reinforcement to 20% increased the compressive yield stress markedly whereas the additional increase to 30 vol.% increased the compressive yield only slightly.

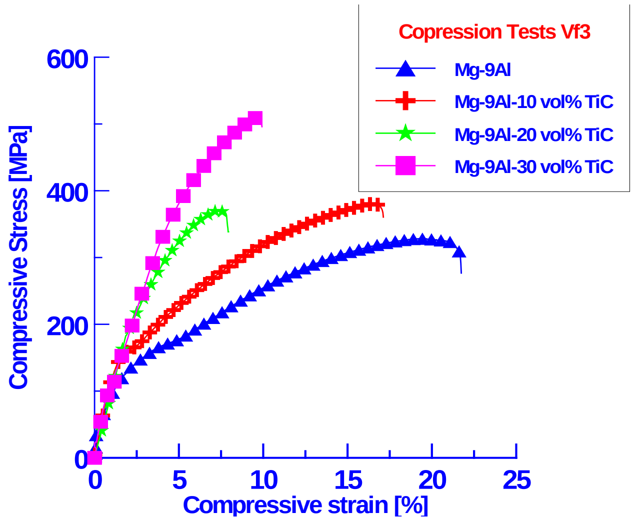

Fig. 6 Compressive stress/strain curves of Mg-9 wt % Al with and without different TiC volume fractions.

The Vickers microhardness of composites reinforced with different TiC volume fractions compared to the base Mg-9 wt % Al material in the as cast, solution heat treated and aged conditions are summarized in Table 2. As was discussed earlier, there were areas with concentrated amounts of TiC. Therefore, it is not surprising that we had 2 sets of values for each specimen corresponding to these differences. Increasing the vol. % TiC in the alloy increased the hardness as expected. The solution heat treatment reduced the microhardness values compared to the as-cast material, presumably due to the reduction of the $Mg_{17}Al_{12}$ interdendritic phases. Likewise, subsequent aging treatments increased the hardness due to precipitation in the Mg dendrites.

TABLE I
SUMMARY OF THE COMPRESSION TESTS FOR MG-9AL AS A FUNCTION OF THE VOL. % TIC

Alloy	Mechanical Properties		
	Yield Stress [MPa]	Ultimate Stress [MPa]	Compressive strain to fracture [%]
0 vol.% TiC	105	330	16.8
10 vol.% TiC	150	380	12.3
20 vol.% TiC	320	450	5.7
30 vol.% TiC	380	510	4.5

TABLE II.
MICROHARDNESS RESULTS FOR MG-9AL WITH DIFFERENT AMOUNTS OF TIC IN AS-CAST, SOLUTION HEAT TREATED AND AGED CONDITIONS

Condition	Microhardness (H_v)			
	0 vol.% TiC	10 vol.% TiC	20 vol.% TiC	30 vol.% TiC
As cast	72			
Solution treated	55	75 108	100 150	122 185
Aged	75	85 106	130 173	140 200

Abrasive wear resistance tests [17] showed the same tendency, namely, increasing TiC vol.% fraction decreased the wear depth in a manner inversely proportional to the hardness values.

IV. SUMMARY

Mg-based MMCs containing 10, 20 and 30 vol. % TiC were produced successfully by mixing TiC+Al powder compacts into liquid Mg. These composites were characterized in the as-cast condition and after solution treating and aging using SEM/EDS, microhardness and compression tests. The following results were obtained:

The Mg dendrites were composed of Mg with around 9 wt.% Al and, during solidification, the TiC particles were rejected to the interdendritic regions. In the interdendritic regions containing the TiC particles, Mg and Al oxides as well as the $Mg_{17}Al_{12}$ intermetallic phase were observed. In certain areas, lower percentages of TiC were observed and, in some cases, the interdendritic regions consisted solely of the $Mg_{17}Al_{12}$ phase. Solution heat treatment reduced the amount of $Mg_{17}Al_{12}$ and oxides, but did not eliminate them. Aging affected the Mg dendrites in a manner similar to the aging effect in Mg AZ91 alloys. Increasing the vol. fraction of TiC reduced the amount of the Mg dendrites without TiC.

Compression tests indicated an increase in the compressive yield strength as well as the maximum compressive strength while the compressive strain decreased with increasing TiC volume fractions. The microhardness also increased with increasing TiC volume fraction in the alloy. Solution heat treatment resulted in a decreased hardness whereas aging increased it to essentially the as-cast values.

There are two types of oxides in the Mg MMCs: small oxide particles in the interdendritic areas and relatively large oxides containing sulphur. The density of the larger oxides increased towards the top of the billet. Significantly, the small oxides clearly preclude large thickness reduction via hot rolling. Thus, it is clear that reducing the oxides in the interdendritic regions is important to improve overall properties and workability of the material

Finally, from a processing standpoint, the stirring system needs to be improved in order that all TiC can be distributed evenly throughout the ingot

ACKNOWLEDGEMENTS

This research was supported by the US Department of Energy under Award Number DE-EE0001100, the North American Die Casting Association and the China Scholarship Council of the Chinese Ministry of Education. The authors would like to thank Vforge Inc. and WPI for performing the semi-solid die casting trials and mechanical tests, respectively. The authors also wish to acknowledge the Electron

Microscopy Laboratory at CSM for making the equipment available or these studies.

REFERENCES

[1]. H. Friedrich and B. Mordike, Technology of magnesium and magnesium alloys in Magnesium Technology - Metallurgy, Design Data, and applications Springer–Verlag, 2006, 219-430.

[2]. E. Aghion and D. Eliezer, EDs. Magnesium 1997 - the First International Conference on Magnesium Science & Technology, The Dead Sea, Nov. 1997.

[3]. E. Aghion and D. Eliezer, EDs. Magnesium 2000 - the Second International Conference on Magnesium Science & Technology, The Dead Sea, Feb. 2000.

[4]. H. Choi, H. Konishi and X. Li," Effects of SiC nanoparticles on mechanical properties and microstructure of cast Mg-12wt.%Al-0.2wt.%Mn nanocomposites, in Magnesium Technology 2011, EDs: W. H. Sillekens, S. R. Agnew, N. R. Neelameggham, and S. N. Mathaudhu, TMS (The Minerals, Metals & Materials Society), 2011 pp. 447 to 452.

[5]. H.Z. Ye and X. Y. Liu, "Review of recent studies in magnesium matrix composites", Journal of Material Science, vol. 39, pp. 6153-6171, 2004.

[6]. H. Capel, S. J. Harris, P. Schulz and H. Kaufman, Mater. Sci. Techn. Vol. 16, 765, 2000.

[7]. Hausmann, C. Cayron, O. Beffort and S. Long, in 9th International Conference on Modern Materials and Technologies, CIMTEC'98, Florence, Italy, June 1998.

[8]. Diw Angi and I. W. Hall, J. Mater. Sci. vol. 27, p. 2093, 1992.

[9]. Y . Kagaw A and E.. Nakata , J. Mater. Lett. Vol. 11, p 176, 1992.

[10]. L. I. Lu, M. O. Lai, M. Gupta, B. W. Chua and A. Osman, J. Mater. Sci. vol. 35, p 5553, 2000.

[11]. S. Nimityongskul, N. Alba-Baena, H. Choi, M. Jones, T. Wood, M. Sahoo, R. Lakes, S. Kou, and X. Li, "Characterization of hot extruded Mg/SiC nanocomposites fabricated by casting", in Magnesium Technology 2011, Eds: W. H. Sillekens, S. R. Agnew, N. R. Neelameggham, and S. N. Mathaudhu, TMS (The Minerals, Metals & Materials Society), 2011, pp. 443 to 446.

[12]. G. Cao, H. Konishi and X. Li, "Mechanical properties and microstructure of Mg/SiC nanocomposites fabricated by ultrasonic cavitation based nanomanufacturing," Journal of Manufacturing Science and Engineering, vol. 130, pp. 31105-1 to 31105-6, 2008.

[13]. G. Cao et al., "Mg-6Zn/1.5%SiC nanocomposites fabricated by ultrasonic cavitation-based solidification processing," Journal of Materials Science vol. 43, pp. 5521–5526, 2008.

[14]. Z. Esen, "TiNi reinforced magnesium composites by powder metallurgy", in Magnesium Technology 2011, Eds: W. H. Sillekens, S. R. Agnew, N. R. Neelameggham, and S. N. Mathaudhu, TMS (The Minerals, Metals & Materials Society), 2011, pp. 457 to 462.

[15]. S. J. B. Reed, Electron Microprobe Analysis, Cambridge University Press, Cambridge, 1977.

[16]. W. Garrett, unpublished work, 2012

[17]. Jo, J. Nuechterlein, W. Garrett, A. Munitz, M.J. Kaufman , J.J. Moore, K. Young , C. Rice, M.M. Makhlouf , D. Apelian, and A. Monroe, SHS die-casting (SHS-DC) of magnesium metal matrix composites (MMCs), to be published in *NADCA, 241 Holbrook*, Wheeling, Illinois, 60090, 2012